Available online at www.sciencedirect.com
ScienceDirect
Defence Technology 12 (2016) 106–112
www.elsevier.com/locate/dt

Measurement of in-bore side loads and comparison to first maximum yaw

Donald E. CARLUCCI [a,*], Ryan DECKER [a], Julio VEGA [a], Douglas RAY [b]

[a] U.S. Army ARDEC RDAR-DSM, Building 94, 2nd Floor, Picatinny, NJ 07806-5000, USA
[b] U.S. Army ARDEC RDAR-EIQ-SB, Building 62, Picatinny, NJ 07806-5000, USA

Received 14 September 2015; revised 11 December 2015; accepted 14 December 2015
Available online 7 January 2016

Abstract

In-bore yaw of a projectile in a gun tube has been shown to result in range loss if the yaw is significant. An attempt was made to determine if relationships between in-bore yaw and projectile First Maximum Yaw (FMY) were observable. Experiments were conducted in which pressure transducers were mounted near the muzzle of a 155 mm cannon in three sets of four. Each set formed a cruciform pattern to obtain a differential pressure across the projectile. These data were then integrated to form a picture of what the overall pressure distribution was along the side of the projectile. The pressure distribution was used to determine a magnitude and direction of the overturning moment acting on the projectile. This moment and its resulting angular acceleration were then compared to the actual first maximum yaw observed in the test. The degree of correlation was examined using various statistical techniques. Overall uncertainty in the projectile dynamics was between 20% and 40% of the mean values of FMY.
Production and hosting by Elsevier B.V. on behalf of China Ordnance Society.

Keywords: Ballistics; Balloting; First maximum yaw; Muzzle exit; Muzzle wear; Projectile dynamics

1. Introduction

In-bore yaw of a projectile in a gun tube has been shown to result in range loss if the yaw is significant [1]. Kent [2,3] and later, Sterne [4], developed the following equations that related in-bore yaw to First Maximum Yaw (FMY).

$$FMY = \left(\frac{2I_T}{I_P} - 1\right)\frac{\delta_{tm}}{\sqrt{1 - \frac{1}{S_g}}} \tag{1}$$

In this equation, I_T and I_P are the projectile's transverse and polar moments of inertia, respectively, S_g is the gyroscopic stability factor, and δ_{tm} is the (small) angle of the projectile in the bore of the weapon at the instant of muzzle exit. We can write this in terms of bore clearance. If we assume that the wheel base of the projectile is determined by the longest distance between the largest diameters of the forward and aft bourrelets (l_{bb}) and assuming small angles, we can write

$$\delta_{tm} \approx \frac{d_{bore} - d}{l_{bb}} \tag{2}$$

where d_{bore} is the diameter of the bore, d is the projectile bourrelet diameter and δ_{tm} is the in-bore yaw in radians. These equations were later implemented and plotted against test results in the experimental firings of Kent and Hitchcock [5].

In 2012, experiments were conducted at Yuma Proving Ground during an effort to determine the effect that severely worn lands at the muzzle of a 155 mm howitzer would have on the range of a projectile [6].

The range loss due to muzzle wear was theorized to come from two sources: pressure loss from escaping propellant gas around the periphery of the projectile and high drag on the projectile, caused by high yaw, due to increased bore clearance.

The pressure loss was determined to be insignificant because the muzzle velocities were well within the expected ranges for the various projectiles fired. Examination and analysis of the high speed video taken during the firings showed very high yaws. When these data were subsequently analyzed, the high yaw-drag alone was confirmed to be responsible for the range loss.

The FMY described in Eq. (1) is physically generated by the spinning of a yawed projectile, irrespective of the gas dynamics about that projectile. If the weapon has a muzzle brake or other

Peer review under responsibility of China Ordnance Society.
* Corresponding author. Tel.: +1 9737242486.
E-mail addresses: donald.e.carlucci.civ@mail.mil; dcarlucci@carlucciarms.com (D.E. CARLUCCI).

http://dx.doi.org/10.1016/j.dt.2015.12.003
2214-9147/Production and hosting by Elsevier B.V. on behalf of China Ordnance Society.

muzzle device, the gas dynamics will likely have more of an effect on the yaw because the projectile is not constrained by the bore during the initial stages of gas ejection.

Measuring the pressure distribution in the muzzle brake is problematic due to the weapon geometry. Pressure gages can easily be placed on the baffle surfaces but determination of the pressure in the flow channels is problematic. Placement of a gage in the flow channels of a muzzle brake has to meet two diametrically opposed criteria: The gage has to remain stationary while hot, high pressure gases blow by it and yet has to be so non-invasive as to not affect the flow. Non-invasive mounting techniques will not survive the gas flow and mounts that are sturdy enough to survive invariably affect the gas flow. Because of this, it was decided to mount twelve pressure transducers, in three sets of four, at a position somewhat up-bore of the muzzle brake. A picture of the mounted gages is shown in Fig. 1.

The shift in the gage locations was maintained to allow the rear two sets to follow the rifling while the forward set was lined up with the center cruciform pattern. In all cases the gages were located at the bottom of the rifling grooves.

The gage placement, so far behind the emergence of the projectile into the muzzle brake, led the team to believe that the best that could be hoped for was a correlation between the net pressure force vector acting on the projectile, at this point in the tube, and the angular location of FMY.

The thought of only obtaining a correlation may be bothersome, but when one considers the difficulty of calculating an exact relation, it is clear why this is all that could be achieved. The first issue is the nature of the pressure side load in-bore. This side load is likely not constant in either space or time. Although we shall display the data as if the loading is constant, one must keep in mind that this represents a temporal integration of pressures acting on fixed-position gages. As the projectile moves through the bore, yawed at some angle, it is rotating. This rotation will cause the pressure “bubble” to rotate as well. The reasoning here is that, if the blow-by is occurring because of wear or damage to the rotating band, this “leak path” must rotate with the band. If a pattern of spiral wear develops in a gun tube, it would tend to support this logic. During transit through the tube, the projectile is constantly trying to resist the rotation about the geometric axis of the bore and trying to spin about its principal (polar) axis. This results in lateral balloting motions and will affect the gas dynamics by changing the cross-sectional area available for blow-by. Finally, as the projectile exits the tube, it will be freed from the constraints of the bore and begin moving due to the projectile and gun dynamics as well as the asymmetric gas ejection and pressure decay on the base. This will cause an additional, non-uniform loading on the base which will impart a moment to the projectile. When one considers all of these factors, which can amplify or cancel one another, it is evident that a correlation is the best that can be hoped for.

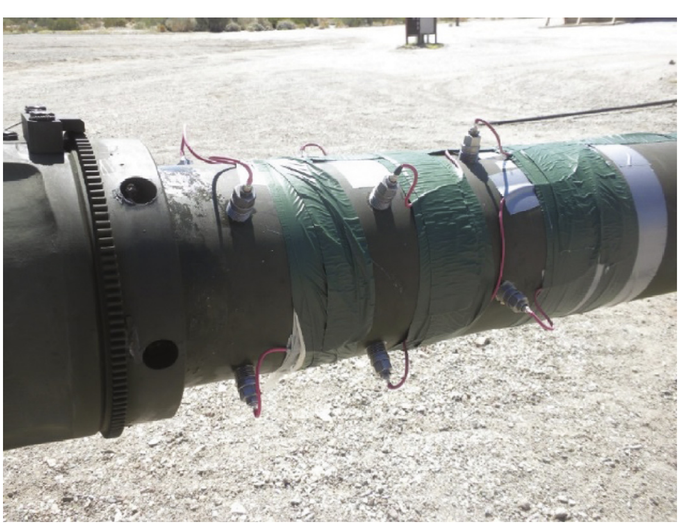

Fig. 1. Pressure transducer locations at muzzle of 155 mm howitzer (muzzle is to the left).

2. Test description

Over the course of several weeks, 1032 projectiles were fired, during which a combination of combustion residue building up in the grooves of the rifling and wearing of the lands of the rifling (known as spiral wear) led to increased blow-by. This increase in blow-by led to a steady increase in the observed FMY as the experiment proceeded, which had the overall effect of gradually decreasing the range of the projectile as described earlier.

3. Pressure data collection

Blow-by pressure was recorded at 10, 15, and 20 inches from the muzzle of the gun tube forming cross sectional planes B, C, and D respectively, each plane containing four pressure transducers 90° apart. The convention used for plane/sensor designation and for the blow-by analysis is as shown below, as viewed toward the muzzle and rotating clockwise starting at 12 o’clock as 0° as shown in Fig. 2. This sensor orientation was configured to determine the blow-by pressure distribution along the side of the projectile in terms of time and was used to calculate the net overturning moment acting on the projectile.

4. Video data reduction

High-speed video was the principal tool used to measure the projectile’s FMY. Traditionally, yaw cards or on-board electronics are used to measure a projectile’s orientation during field testing. Since it was desired to quantify the maximum range loss, the team was required to shoot at a quadrant elevation of 800 mils (45°), making it impossible to place yaw cards in the necessary locations. Due to the significant costs associated with on-board electronics, telemetry systems were used on only a few of the 1032 projectiles fired during the test.

To measure the FMY in a cost-effective manner, the testing team leveraged a new developmental technology called the Automated Launch Video Analysis (ALVA) method [7]. The ALVA system works by capturing video from two opposing high speed camera systems (with rotating views) located roughly 35 m downrange. Computer vision algorithms then extract the projectile shape in every video frame as illustrated in the flight image shown on the left of Fig. 3. The orientation of the projectile shape is then determined as observed from each

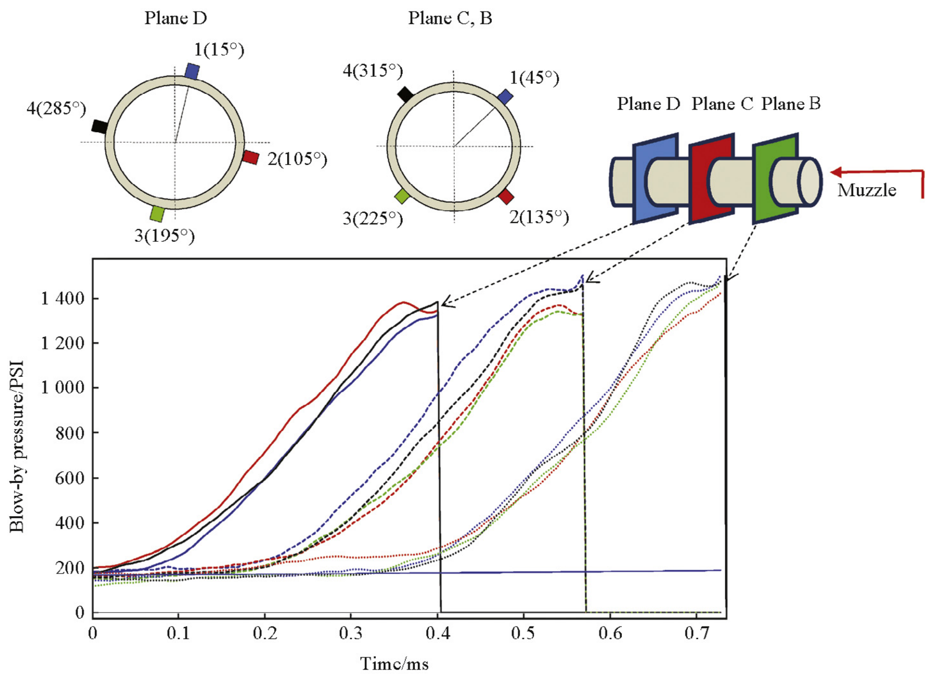

Fig. 2. Sensor setup and blow-by pressures at locations B, C and D.

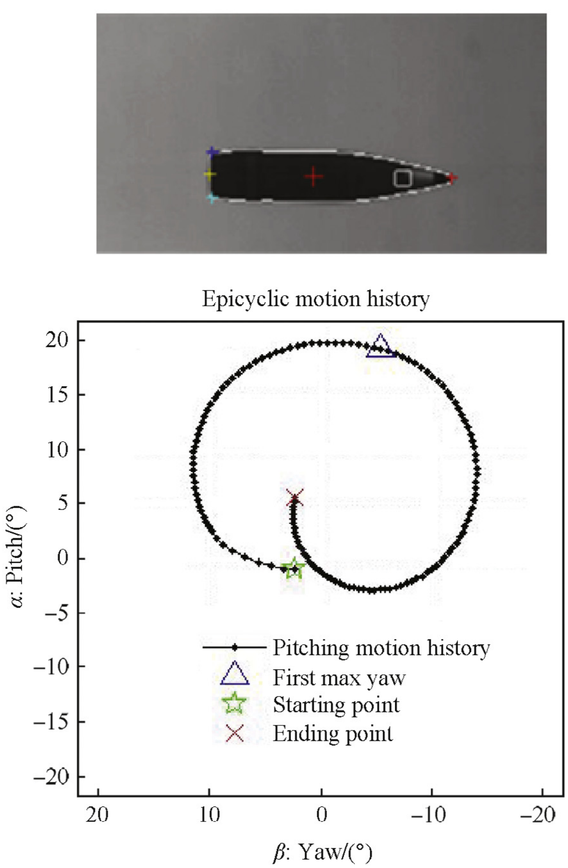

Fig. 3. Projectile shape segmentation (left) and initial orientation history (right) (from Ref. 7).

camera throughout each video. Finally, the geometry of the range layout is considered along with the synchronized pitching motion histories estimated from each individual camera and the results are resolved into a single 3D motion history. One of the unfiltered orientation history plots that results entirely from the video analysis is shown on the right side of Fig. 3. Although only one nutation cycle was captured during this effort, subsequent tests have captured as many as three nutation cycles, from which aeroballistic characterization data can be extracted [8]. Only a single nutation cycle is sufficient to measure the FMY for each shot, as it represents the maximum angle of attack observed during the first epicycle.

The results of all rounds analyzed from this test are shown in Fig. 4 [9]. As expected, the measured FMY and range loss have

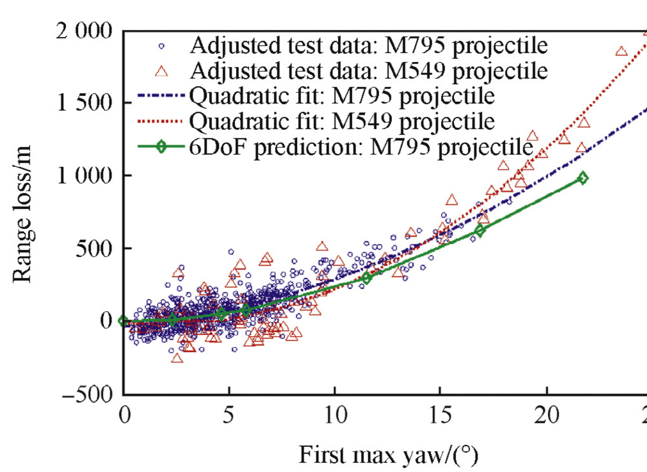

Fig. 4. Relationship between FMY and range loss (from Ref. 9).

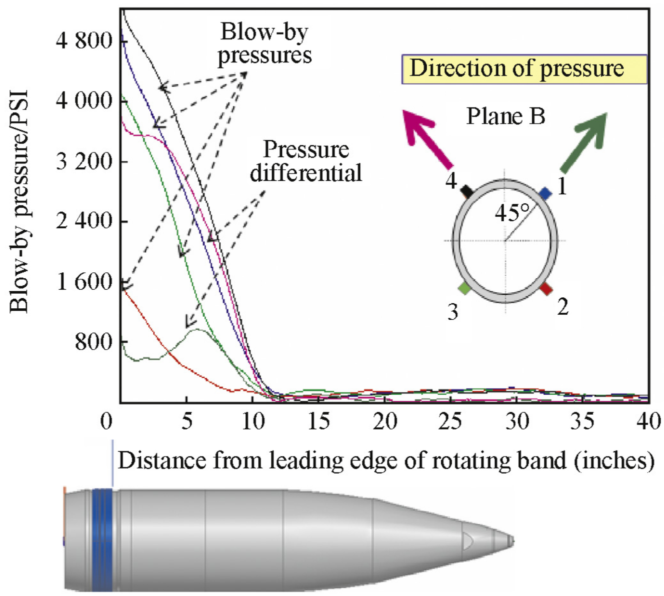

Fig. 5. Plane B – Blow-by pressure distribution along the side of the projectile.

a quadratic relationship. In addition, the observed trend closely matched aeroballistic predictions from a study of the M795 projectile using the GTRAJ simulation software package.

5. Pressure data analysis

As discussed earlier, an arrangement of pressure transducers was positioned on the cannon tube near the muzzle of the weapon. An analysis of the differential pressures recorded on the four-adjacent pressure readings was conducted to determine the net force acting on the projectile. Of the 1032 rounds fired during this test, 29 samples were selected from various levels of spiral wear for the differential pressure analysis. Pressure data from plane B were selected for determination of the overturning moment because it was the closest to the muzzle of the gun tube.

6. Blow-by pressure distribution along the side of the projectile

DADISP 6.5 and its data reduction tools were used to process the blow-by pressure data and perform mathematical operations to obtain the net differential pressure across the projectile. As a first step, the pressure vs time data were converted into pressure vs projectile travel distance. This was done through knowledge of the projectile velocity at the muzzle. Since the pressures behind the rotating band were assumed to be relatively uniform, the blow-by data starting point was chosen as the leading edge of the projectile rotating band. A sample of the blow-by pressure distribution calculated along the side of the projectile is shown in Fig. 5.

7. Net overturning moment acting on the projectile

The pressure distribution was used to calculate the net force acting on the side of the projectile. This net force was then integrated and the plane in which it acts, passing through the CG of the projectile, was determined. The results of this calculation were the magnitude and direction of the overturning moment that would cause the projectile to yaw in the bore, a sample of which is shown in Fig. 6 and Table 1. This moment is counteracted by the tube while the projectile is in bore but is relieved over a very short time as the projectile exits the muzzle. At the very least, the projectile will exit the tube with a yaw angle admitted by the clearance between the bourrelets and the I.D. of the rifling. The proper way to model the dynamics associated with this complex release process remains to be examined. The moment, as calculated above, was used as an initial attempt at determining the analytical location and

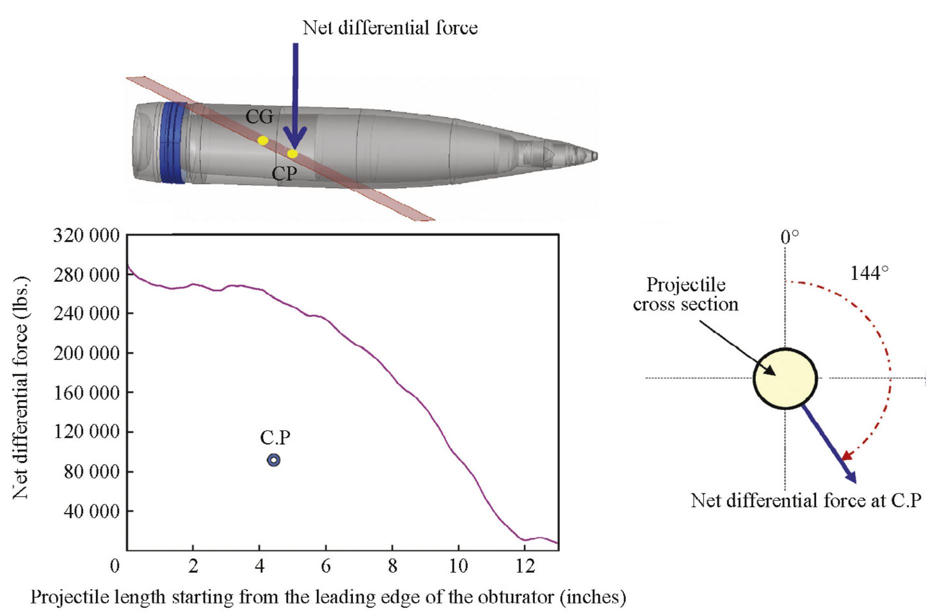

Fig. 6. Overturning moment acting on the projectile.

Table 1
Detailed data from calculations in Fig. 6.

Parameter	Calculation
X_cg/inches	4.7
Y_cg/inches	114,827.7
Area under the curve/lb-inch	2,368,970.3
Torque distance/inches	2.5
Torque/lb-inch	5,869,466.5
Torque/(32.2*12)/lb-inch	15,190.1
Angle/degrees	144
Cross sectional area/inch^2	74.2

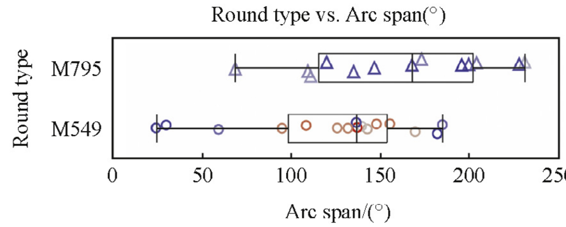

Fig. 8. Arc span by round type.

magnitude of FMY. Thus, the best that could be hoped for was a correlation with an analytic result.

The direction of the net-pressure force from the 29 rounds analyzed using this method was then computed and expressed as an angle from 0 to 360 degrees in a counter-clockwise direction when looking from the breech toward the muzzle of the gun. Note that this was changed from the way it was originally collected to use the same coordinate system employed by the aeroballisticians. In this convention, a pressure acting to the right would have a value of zero degree.

Using this same convention, the projectile pointing direction (not FMY magnitude) was calculated at the location of the FMY for each of the 29 rounds analyzed. When plotted in Fig. 7, the relationship between the net direction of the blow-by pressure force clearly has some correspondence to the projectile's pointing orientation at FMY. In the figure, the red dots indicate the angle of the net pressure force, and the green triangles represent the direction of the FMY. The blue arc-span lines are shown to indicate which pressure angle corresponds to which FMY orientation. The radial scaling is arbitrary and was chosen for illustration purposes only.

The results from this analysis show that on average for the 29 rounds investigated, the average arc-span between the net angle of blow-by force and the projectile's orientation was roughly 140° in the clockwise direction. This is interesting because aeroballistic simulations of an M795 155 mm projectile fired at the expected muzzle velocity predict that the projectile's orientation during the first epicycle should rotate 104° between muzzle exit and the FMY (similar to the plot shown on the right in Fig. 3). This suggests that the projectile is under-rotating (not under-spinning) by roughly 37°. Given the twist rate of the M777 is 1 revolution in 20 calibers, this 37° gap is likely caused by the fact that there is roughly a 0.3 m distance in the cannon tube between the muzzle and the location where the pressure transducers are located as shown in Fig. 1, theoretically resulting in about 34 degrees of rotation.

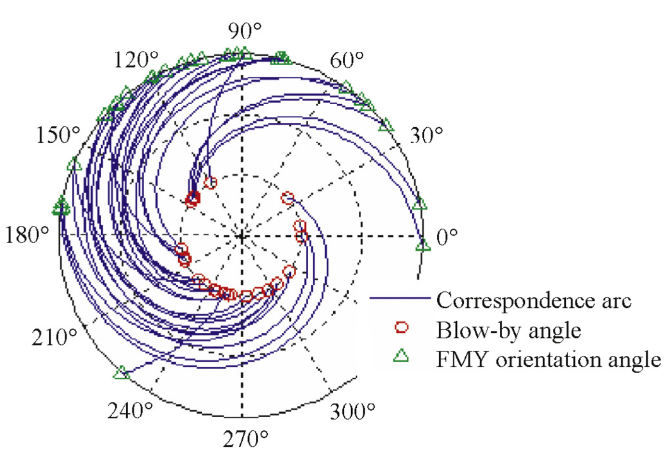

Fig. 7. Illustration of correspondence between net pressure angle and FMY orientation.

Given the method for measuring the values of both net pressure blow-by force angle as well as estimating the true orientation at FMY, it is impressive that the standard deviation of the arc-span lengths is only roughly 52° (14.4% of a complete circle).

Figs. 8 and 9 illustrate the distribution of arc spans for the 29 rounds. In both figures, the data are colored based on the FMY values (blue to gray to red, ascending). Fig. 8 shows the arc span values by round type, indicating that the rounds behaved similarly, although the M795 had slightly higher arc spans on average. Fig. 9 shows the individual arc spans for the 29 rounds, which serves to illustrate the relatively consistent rotation from round to round throughout the test. The histogram and fitted normal curve on the right of Fig. 9 characterize the distribution of the arc spans for all observations. The normal quantile plot shows that the arc span data follow a normal distribution, an important finding given the number of variables represented, including the round type, and the test sequence (associated with gun wear).

8. Statistical analysis

Using least-squares regression to predict the FMY orientation based on measured blow-by angles by round type gives a model which explains about 1/3 of the variation in the FMY values observed (Fig. 10), with a 45 degree standard deviation for the M549 and a 30 degree standard deviation for the M795. However, a more detailed multiple regression analysis shows the "round type" factor to be non-significant in terms of predicting FMY and this potential explanatory variable was removed from the model. Therefore, a "penalized" regression method (Fig. 11) called LASSO (Least Absolute Shrinkage and Selection Operator) [10] was used to predict FMY from blow-by orientation using an assumed Cauchy distributed regression model.

In this case, a Cauchy distribution was selected based on the fact that there are many unquantified variables which are expressing themselves and "random variation" or noise in this

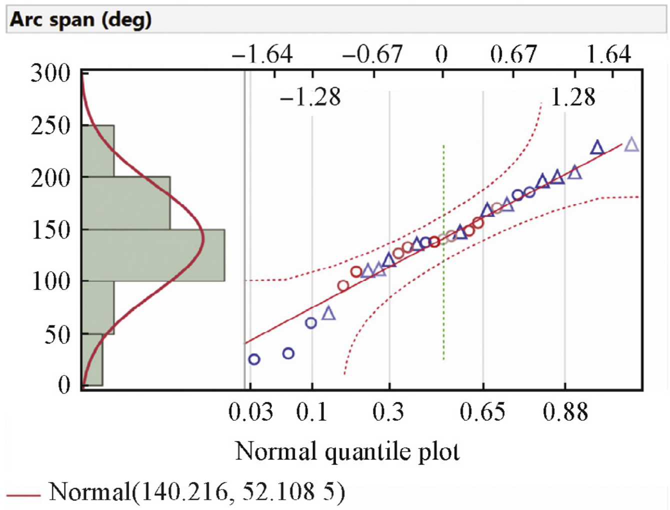

Summary statistics

Mean	140.21566
Std Dev	52.108542
Std Err Mean	9.6763133
Upper 95% Mean	160.03668
Lower 95% Mean	120.39463
N	29

Fig. 9. Arc span vs sample number, and data distribution with fitted normal curve.

Generalized regression

Adaptive lasso with AICc validation

Model summary

Response	FMY orientation/(°)
Distribution	Cauchy
Estimation method	Adaptive lasso
Validation method	AICc
Location model link	Identity
Scale model link	Identity

Measure	Training
Number of rows	29
Sum of frequencies	29
−LogLikelihood	146.61447
BIC	303.33083
AICc	300.18894
Generalized Rsquare	0.5898354

Estimation details

Number of grid points	150
Minimum penalty fraction	0
Grid scale	Linear

Parameter estimates for original predictors

Term	Estimate	Std error	Wald Chisquare	Prob> Chisquare	Lower 95%	Upper 95%
Intercept	−26.95139	16.483408	2.6734276	0.1020	−59.25828	5.3554929
Blow-by angle/(°)	0.5097806	0.0581089	76.962932	<0.0001*	0.3958893	0.6236719
Scale	16.734193	4.3482884	14.810608	0.0001*	8.2117048	25.256682

Prediction profiler

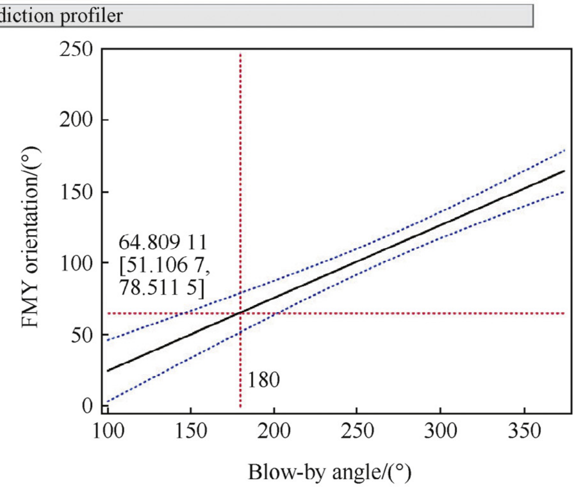

Fig. 11. Cauchy regression analysis of blow-by angle vs FMY.

dataset. The Cauchy distribution is an appropriate method to deal with this inflated error. Sources of variation, unquantified in this study, include the muzzle pointing angle, muzzle crossing velocity, center of gravity jump, aerodynamic jump, instrumentation repeatability, environmental effects, fouling, etc. The Cauchy regression model shows that 59% of the variation in the FMY orientation is predicted by the blow-by angle, while 41% of the variation is noise, or those other variables not quantified by the regression model (Fig. 11).

Fig. 12 shows the FMY magnitude predictions based on blow-by torque by round type which shows markedly different

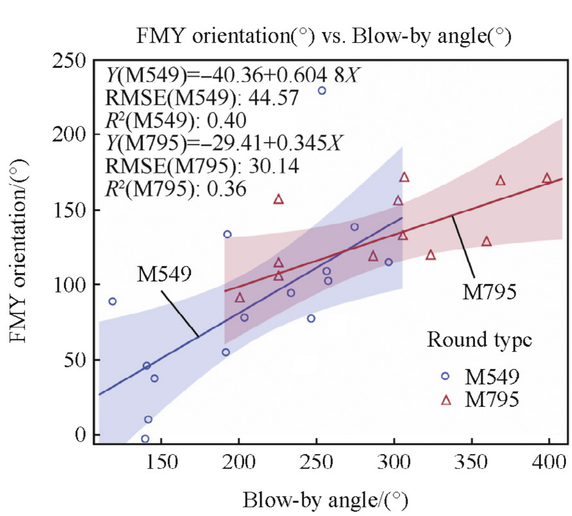

Fig. 10. Blow-by angle vs FMY orientation by round type.

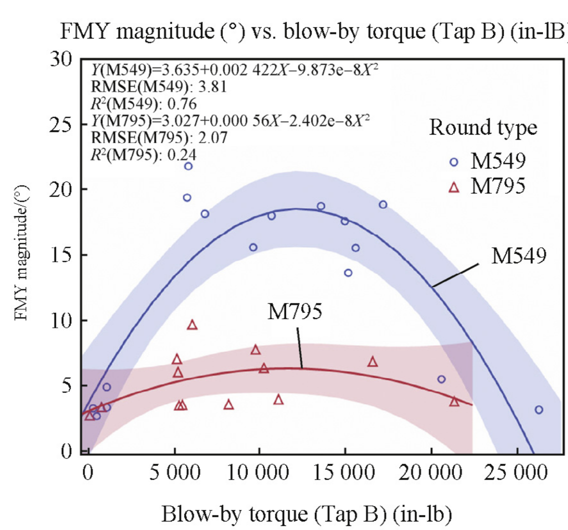

Fig. 12. Comparison of blow-by torque vs FMY magnitude.

behavior between the M795 (relatively flat/weak relationship) and the M549 (highly curved, relatively strong relationship). The blow-by torque explains 76% of the variation in the FMY magnitude data for the M549, while for the M795 it explains only about 20%.

9. Conclusions

In-bore yaw of a projectile was successfully inferred using pressure transducers mounted near the muzzle of a 155 mm gun tube. The data collected were integrated to determine a net overturning moment on each projectile. Comparison of these data with the aeroballistic models and observations of FMY obtained from video analysis showed distinct scatter in the data but the mean value is close to predictions. Subsequent statistical analysis determined that the variation was approximately 40% of the mean. This indicates that any calculations performed to determine the dynamic motion of a 155 mm projectile will have approximately this much error. There were distinct differences between the correlation of the M549 projectile and the M795 projectile to the calculated overturning moment. In the former case 76% of the variation in range was correlated to the overturning torque, while in the latter case only 20% of the variation correlated. We can conclude from this that the overturning moment has a greater effect on the M549 range than it does the M795. The balance of the scatter is attributed to phenomena which were not measured in these experiments such as weapon movement, projectile principal axis offset, etc. There is a great deal of information that still need to be uncovered before any prediction of projectile exit dynamics can become more exacting.

References

[1] Breger M.P., Morrison C.C. (Transl.). Position and form of bands for projectiles. Notes on the Construction of Ordnance, No. 27. Washington, DC; 10 June 1884.

[2] Kent RH. An elementary treatment of the motion of a spinning projectile about its center of gravity. Ballistics Research Laboratory Report No. 85. Aberdeen Proving Ground, MD; 1937.

[3] Kent RH, McShane EJ. An elementary treatment of the motion of a spinning projectile about its center of gravity. (Revised Ballistics Research Laboratory Report No. 85), Ballistics Research Laboratory Report No. 459. Aberdeen Proving Ground, MD; April 1944.

[4] Sterne TE. On jump due to bore clearance. BRL Report No. 491. Aberdeen Proving Ground, MD; 28 Sept. 1944.

[5] Kent RH, Hitchcock HP. Comparison of predicted and observed yaw in front of the muzzle of a 12” gun. Report No. 990 AD-116-140. USA BRL, Aberdeen Proving Ground, MD; July 1956.

[6] Dickerson MK Establishment of 155-mm cannon condemnation criteria from interior ballistic test projectile characterization. YTC No. 12-RD-0648-L5. U.S. Army Yuma Proving Ground, Yuma Test Center, Munitions and Weapons Division, Yuma, Arizona 85365-9498, ATEC Project No. E0674; 27 December 2012.

[7] Decker R, Kolsch M, Yakimenko OA. An automated method for computer vision analysis of cannon-launched projectile video. J Test Eval 2014; 42(5):1248–56.

[8] Decker R, Duca M, Hooke R. Aerodynamic coefficient measurement using launch video analysis of sabot-equipped projectiles. In: Proceeding of the 2014 joint classified ballistics and warheads symposium, Monterey, CA; August 2014.

[9] Decker R, Yakimenko OA, Kolsch M. Artillery pitch and yaw measurement test report: an automated video analysis method to measure first maximum yaw. ARMET-TR-13026. U.S. Army Armament Research, Development, and Engineering Center, Picatinny Arsenal, NJ; May 2014.

[10] Tibshirani R. Regression shrinkage and selection via the lasso. J. R Stat Soc B 1996;58(1):267–88.